



The origin of neural stem cells impacts their interactions with targeted-lipid nanocapsules: Potential role of plasma membrane lipid composition and fluidity

Dario Carradori^{a,d}, Andreia G. dos Santos^b, Julien Masquelier^c, Adrien Paquot^c, Patrick Saulnier^d, Joël Eyer^d, Véronique Préat^a, Giulio G. Muccioli^c, Marie-Paule Mingeot-Leclercq^b, Anne des Rieux^{a,*}

^a Université catholique de Louvain, UCLouvain, Louvain Drug Research Institute, Advanced Drug Delivery and Biomaterials, Avenue E. Mounier 73, 1200 Brussels, Belgium

^b Université catholique de Louvain, UCLouvain, Louvain Drug Research Institute, Cellular and Molecular Pharmacology, Avenue E. Mounier 73, 1200 Brussels, Belgium

^c Université catholique de Louvain, UCLouvain, Louvain Drug Research Institute, Bioanalysis and Pharmacology of Bioactive Lipids, Avenue E. Mounier 72, 1200 Brussels, Belgium

^d Université d'Angers, Unité de Micro et Nanomédecines Translationelles (UMR INSERM 1066/CNRS 6021), Institut de Biologie en Santé PBH-IRIS, CHU Angers, 49033 Angers, France

ARTICLE INFO

Keywords:

Fluidity
Lipid composition
Lipid nanocapsules
Neural stem cells
NFL-TBS.40-63
Permeability
Plasma membrane

ABSTRACT

The adsorption of a peptide (NFL-TBS.40–63 peptide (NFL)) known to induce neural stem cells (NSC) differentiation in vitro, at the surface of lipid nanocapsules (LNC) provides a targeting drug delivery system (NFL-LNC) that penetrates subventricular zone-neural stem cells (SVZ-NSC) but not central canal-NSC (CC-NSC). We hypothesized preferential interactions could explain, at least partially, the different properties of SVZ- and CC-NSC plasma membranes. The objective of this work was to compare SVZ- and CC-NSC plasma membrane lipid composition, fluidity and permeability. Plasma membranes of SVZ- and CC-NSC were isolated and analyzed by LC-MS for their lipid content. Membrane fluidity was evaluated by measuring the generalized polarization (GP) of Laurdan and membrane permeability by fluorescent dextran penetration. Liposomes with different lipid compositions and steady state fluidities were prepared. ΔGP was measured after incubation with NFL-LNC. A significantly higher proportion of cholesterol, ceramides, sphingomyelins, phosphatidylethanolamines and a lower proportion of phosphatidylcholines and sulfatides were observed in SVZ- compared to CC-NSC. Fluidity, probably more than lipid composition, drove NFL-LNC and NSC interactions, and SVZ-NSC were more sensitive to NFL permeabilization than CC-NSC. We demonstrated that NSC membrane lipid composition and fluidity depended of NSC origin and that these features could play a role in the specific interactions with NFL-LNC.

1. Introduction

The in situ differentiation of endogenous neural stem cells (NSC) remains one of the most promising strategies for the treatment of central nervous system (CNS) disorders. This technique would avoid both transplantation-associated issues (e.g., cell sources and cell viability) [1] and procedural limitations derived from the in vitro manipulation of exogenous NSC (e.g., the cultivation under restricted conditions and the risk of genetic modifications) [2]. Although many drugs and drug delivery systems have been tested in vivo to induce in situ differentiation of endogenous NSC [3,4], no treatment based on this strategy has yet reached the clinic [5]. Indeed, the lack of NSC-targeting molecules is a limitation to in situ NSC differentiation

strategies as non-selective systems might present off-target associated side-effects or inefficiencies.

The 24-aminoacid peptide NFL-TBS.40-63 (NFL), corresponding to the tubulin-binding site of the neurofilament light subunit [6], showed a strong interaction with NSC of the subventricular zone (SVZ-NSC) of the brain [7]. In vitro, NFL massively penetrated SVZ-NSC by direct translocation and induced NSC differentiation while in vivo, NFL localized in SVZ-NSC niches after intra-lateral ventricular injections in the rat brain. NFL was not detected in astrocytes and neurons and showed no toxicity in vitro and in vivo [8,9].

To form a drug delivery system that specifically targets NSC, NFL was adsorbed via ionic and stable interactions at the surface of lipid nanocapsules (LNC) to form NFL-LNC [10,11]. NFL is a 2.7 kDa peptide

* Corresponding author.

E-mail address: anne.desrieux@uclouvain.be (A. des Rieux).

<https://doi.org/10.1016/j.jconrel.2018.11.005>

Received 16 July 2018; Received in revised form 1 October 2018; Accepted 4 November 2018

Available online 05 November 2018

0168-3659/ © 2018 Elsevier B.V. All rights reserved.

with a positive charge (+2) at pH7, an extinction coefficient of $3840 \text{ M}^{-1} \text{ cm}^{-1}$ and isoelectric point at pH 10.38. NFL is poorly soluble in water, consequently it is recommended to use sonication after dissolution in any aqueous solvents and low-concentration working-solutions ($\leq 1 \text{ mM}$). LNC are a versatile drug delivery system with high potential for clinical translation. LNC have a long shelf life (> 18 months), the ability to deliver both lipophilic and hydrophilic drugs and a high biocompatibility [12]. These particles are produced by a solvent-free method and have a lipid core of caprylic/capric triglycerides (Labrafac®) and a shell of lecithin (Lipoid®) with PEG₆₀₀/PEG stearate derivatives (Kolliphor®), all approved by the FDA [12]. We have previously found that NFL-LNC showed a strong interaction with SVZ-NSC but not with NSC located in the central canal (CC-NSC) of the spinal cord [11]. As the SVZ-NSC interactions were not affected by low temperature (4 °C), ATP depletion or pre-incubation with NFL alone, NFL-LNC interacted with NSC by an energy-independent mechanism that was not mediated by a receptor [11].

We thus hypothesized that different plasma membrane properties of NSC originating from different niches could impact nanomedicine, and more particularly NFL-LNC, interactions with NSC. Therefore, we focused our attention on NSC plasma membrane lipid composition and fluidity. For the first time, to the best of our knowledge, we showed that depending of the localization of NSC in the CNS, the lipid composition and the fluidity of their membrane was different. We also observed that not only SVZ-NSC and CC-NSC membrane steady state fluidity was different, but also that a direct correlation can be observed between steady state fluidity of NSC membrane and its modulation by NFL-LNC.

2. Materials and methods

2.1. Materials

Biotinylated NFL-TBS.40-63 (NFL) was purchased from GeneCust (Luxembourg, Luxembourg). Labrafac® was purchased from Gattefosse SA (Saint-Priest, France). Lipoid® was purchased from Lipoid GmbH (Ludwigshafen, Germany). Kolliphor HS® was purchased from Sigma (Saint-Louis, Missouri, USA). Sodium chloride (NaCl) was purchased from Prolabo (Fontenay-sous-bois, France). Egg sphingomyelin (eSM), 1-palmitoyl-2-oleoyl-*sn*-glycero-3-phosphocholine (POPC), egg ceramide (eCE) and cholesterol (Chol) were purchased from Avanti Polar Lipids (Birmingham, Alabama, USA). 6-dodecanoyl-2-dimethyl-aminonaphthalene (Laurdan) was purchased from Molecular Probes (Carlsbad, California, USA). HEPES (1 M), Penicillin/Streptomycin (10,000 U/mL) (Pen/strep), Na Pyruvate (100 mM), B27 (50×), MEM alpha (no nucleosides), 0.05% Trypsin-EDTA (1×), DNase (1 U/mL) were purchased from Thermo Fisher Scientific (Waltham, Massachusetts, USA). Hyaluronidase (1 mg/mL) and FITC-Dextran (FD) 4 and 10 kDa were purchased from Sigma (Saint-Louis, Missouri, USA). EGF and bFGF were purchased from Peprotech (London, UK). BD CellTak was purchased from Corning Inc. (New York, New York, USA).

2.2. Isolation of neural stem cells

The isolation of NSC ($N = 9$) was performed according to Directive 2010/63/EU under the guidelines of the Belgian Government following the approval by the ethical committee for animal care of the health science sector of the University catholique de Louvain. For each isolation, SVZ-NSC and CC-NSC came from the same animals. NSC were cultivated as floating neurospheres, which appeared after 5 days, and used at 7 days after isolation.

SVZ-NSC were isolated according to Guo et al. [13] and CC-NSC according to the protocol developed by Hugnot et al. [14]. SVZ-NSC were seeded at 2×10^5 to 3×10^5 cells/T75 flask in 12 mL of cell culture medium (1.25 mL of D-glucose 1 M, 750 µL of HEPES, 500 µL Pen/Strep, 500 µL Na Pyruvate, 500 µL of B27 and 10 ng/mL of EGF in 50 mL of MEM alpha no nucleosides medium). CC-NSC were seeded at

2×10^5 to 3×10^5 cells/T75 flask in 12 mL of cell culture medium (identical to SVZ-NSC supplemented with 10 ng/mL of bFGF). Nestin is a marker commonly used to identify NSC [15]. Thus, the proportion of undifferentiated NSC primary cell cultures was evaluated by measuring the percentage of Nestin⁺ cells by FACS after neurosphere dissociation [11]. In average, 75% of the cells were positive for Nestin, which is in the range of what has been reported in the literature for NSC primary cultures [7,11]. Neurospheres are heterogenous structures mostly made of progenitor cells at different stages of differentiation. So, even if the remaining 25% were not identified, they could be progenitor cells or NSC in the process of differentiating. In consequence, our results mainly relate to NSC but the influence of cell differentiation stage cannot be excluded.

2.3. Isolation of neural stem cell plasma membranes

The isolation of NSC plasma membrane ($N = 5$) was performed according to Susky et al. [16]. Briefly, 5×10^7 SVZ-NSC or CC-NSC were collected in a 50 mL falcon and centrifuged for 5 min at 500g. Supernatants were discarded, and 200 µL of lysis buffer (730 mM sucrose, 20 mM Tris-HCl, 100 µM EDTA) were added. The cells were left on ice for 30 min. Then, 30 mL of milliQ water were added, and the tube was kept on ice for another 30 min. Then the samples underwent a series of centrifugation steps. The samples were centrifuged for 5 min at 800g and the supernatants were recovered and centrifuged again for 5 min at 800g. The supernatants were transferred in a 3137–0050 Oak Ridge tube and centrifuged for 10 min at 10000g (rotor JA-20, Beckman). The supernatants were recovered and centrifuged for 10 min at 10000g. Then, the supernatants were transferred to new tubes and further centrifuged at 25000g for 20 min. The pellets were resuspended in 15 mL of ice-cold starting buffer (225 mM mannitol, 75 mM sucrose, and 30 mM Tris-HCl) and centrifuged for 20 min at 25000g. The pellets were recovered in 0.5 mL of plasma membrane resuspension buffer (5 mM Bis-Tris and 0.2 mM EDTA, pH 6), placed on top of a sucrose gradient (from the bottom: 3 mL of sucrose 53%, 4 mL of sucrose 43%, and 4 mL of sucrose 38% dissolved in water) in an Ultra-Clear centrifuge tube and centrifuged for 2 h 30 min at 95000g (rotor SW40, Beckman). Centrifugation on the sucrose gradient resulted in three bands (from the bottom: plasma membrane, mitochondria, and plasma membrane-associated microdomains). Top and bottom bands were recovered using a pipette and pooled. The bands were diluted up to 1 mL in starting buffer.

2.4. Lipid composition of neural stem cell plasma membranes

Cholesterol (both free and ester forms) concentration was determined by the Amplex® Red Cholesterol Assay Kit ($N = 5$) (Thermo Fisher Scientific) according to the manufacturer's instructions. The relative abundance of the plasma membrane lipids was determined by HPLC-MS ($N = 5$) after extraction of the lipids from the plasma membrane in the presence of adequate internal standards as previously described [17,18]. Briefly, the lipid fractions were analyzed using a LTQ-Orbitrap mass spectrometer (Thermo Fisher Scientific) coupled to an Accela HPLC system (Thermo Fisher Scientific). Analyte separation was achieved using a C-18 Supelguard pre-column and a Kinetex LC-18 column (5 µm, 4.6 × 150 mm) (Phenomenex). Three mobile phase systems were used depending on the lipids analyzed: (i) phosphatidylcholines, and sphingomyelins; (ii) phospholipids and sulfatides; and (iii) ceramides [18]. For each lipid, the data are expressed as a ratio of area under the curve (AUC) of the lipid of interest over the AUC of the internal standard.

2.5. Preparation of liposomes

Liposomes were made according to Hope et al. ($N = 4$) [19]. The amount of lipids and Laurdan required to reach a final concentration of

Table 1
Liposome composition.

Liposomes	POPC (%)	eSM (%)	Chol (%)	eCE (%)
1	10	30	–	60
2	60	30	–	10
3	33	33	33	–
4	15	70	15	–
5	70	15	15	–
6	15	15	70	–
7	0	50	50	–
8	50	50	0	–
9	50	0	50	–
10	50	25	25	–
11	25	50	25	–
12	25	25	50	–

Egg ceramides (eCE), Egg sphingomyelins (eSM), 1-palmitoyl-2-oleoyl-*sn*-glycero-3-phosphocholine (POPC), and cholesterol (Chol). %, mM %.

10 and 0.01 mM, respectively, was dissolved in 1 mL of chloroform. After drying the lipid mixture with nitrogen, the lipid film was placed overnight in a vacuum desiccator to remove remaining solvent traces. The lipid film was hydrated with 1 mL of phosphate-free buffer (10 mM Tris, 0.1 M NaCl, pH7) and incubated at 50 °C for 30 min. The suspension was subjected to five cycles of freezing/thawing to obtain multilamellar vesicles. Liposomes were obtained by extrusion (x20) through poly carbonate filters (Nucleopore Track-Etch Membrane Whatman®, Brentford, UK) with a pore diameter of 0.1 μm. Phospholipid concentrations were determined according to the protocol developed by Bartlett [20]. Liposomes were stored at 4 °C and used within 2 days following preparation. Different lipid molar ratios of POPC/eSM/eCE (Liposomes 1–2) and Chol/POPC/eSM (Liposomes 3–12) were used (Table 1). It was not possible to form liposomes with the composition selected for Liposome 6 so this formulation was excluded. Regardless of the lipid composition, liposomes had a mean diameter of 146 nm with a PDI of 0.160 and a ζ-potential of –7.5 mV were generated [21,22].

2.6. Measurement of liposome plasma membrane fluidity

Liposome fluidity (N = 4) was studied by measuring the general polarization (GP) of Laurdan, a fluorescent probe sensitive to polarity and lipid packing, according to the method described by Parasassi et al. [23]. The liposomes were diluted 1/10 in 1 mL HBSS (final lipid concentration, 1 mM) and placed into a fluorometric cuvette with a 10-mm optical path length. Laurdan emission spectra were recorded at 25 °C using $\lambda_{ex} = 360$ nm, and $\lambda_{em} = 440$ nm (emission in blue, I_B) and 490 nm (emission in red, I_R), where I_B and I_R are the fluorescence intensities emitted by Laurdan in the gel phase and liquid crystalline phase, respectively. GP was calculated using the following formula: $GP = (I_{440} - I_{490}) / (I_{440} + I_{490})$. The higher the GP, the more rigid the membrane and consequently, the lower the GP the more fluid the membrane.

2.7. Preparation of NFL-LNC and influence on liposome plasma membrane fluidity

LNC were prepared according to Heurtault et al. [24]. Briefly, 0.846 g Kolliphor HS®, 0.075 g Lipoid®, 0.089 g NaCl, 1.028 g Labrafac® and 2.962 mL of water were mixed under magnetic stirring for 5 min at 40 °C. Temperature cycles (a minimum of 3) of progressive heating/cooling were done between 60 °C and 90 °C to cross the so-called emulsion inversion zone. During the cooling phase of the last cycle and at 74 °C (in the phase inversion zone), 12.5 mL of water (4 °C) were added under high-speed stirring. The nanoparticles were filtered on a 0.22-μm filter to increase their microbiological stability during storage and to avoid the risk of any possible microorganism contamination

during the course of the experiments. NFL-LNC were produced by incubating 369 μL of 1 mM NFL solution (in water) overnight with 1 mL of stock-LNC under gentle stirring. NFL-LNC had a size, PDI and ζ-potential of 65 nm ± 4, 0.2 and – 7.45 mV ± 5, respectively [11].

NFL-LNC impact on liposome membrane fluidity was evaluated by the measure of GP of Laurdan and ΔGP. GP of liposomes (N = 3 for Liposome 1 and Liposome 2, N = 4 for Liposome 3–5 and Liposome 7–12) were measured before and after incubation with 1.26 mg/mL of NFL-LNC. Of note, for liposome 6 we could not obtain a reliable measure of GP. ΔGP was calculated as follow: $\Delta GP = GP_{steady\ state} - GP_{after\ treatment}$. In the range of the GP measured in these experiments, when ΔGP increased, that reflected a fluidification of the membrane and a rigidification when it decreased.

2.8. Influence of NFL-LNC on neural stem cell plasma membrane fluidity

NSC plasma membrane fluidity was evaluated by measuring GP of Laurdan (N = 4). Briefly, 1×10^6 /mL of SVZ-NSC or CC-NSC were incubated with 1% BSA for 5 min and then centrifuged at 500 g for 5 min. The cells were resuspended in 2.5 μM Laurdan in HBSS and incubated for 5 min at room temperature. NSC were centrifuged again at 500 g for 5 min and suspended in HBSS at 1×10^6 /mL. GP (N = 4) was recorded before and after 5-min incubation with 1.26 mg/mL of NFL-LNC as described in 2.6.

2.9. Sensibility of neural stem cell plasma membrane to NFL permeabilization

The impact of NFL on NSC plasma membrane permeability was analyzed by measuring the variation of fluorescence before and after incubation with different concentrations of NFL (2.7, 10 and 20 μM) followed by incubation with FITC-Dextran 4 kDa (FD4) and 10 kDa (FD10) (N = 3). SVZ- and CC-NSC neurospheres were incubated with NFL for 5 min at 37 °C and then washed 3 times in FD-free medium before incubation with FD4 and FD10 (20 μM) for 10 min at 37 °C. The neurospheres were washed, dissociated and analyzed by FACS.

FD penetration in SVZ-NSC was also analyzed by confocal microscopy (Zeiss Cell Observer Spinning Disk microscope, Carl Zeiss). After incubation with NFL and FD, neurospheres were washed 3 times with PBS and fixed with 4% PFA for 15 min. They were mounted with VECTASHIELD® antifade mounting medium and 2 pictures/condition were randomly acquired.

2.10. Statistical analyses

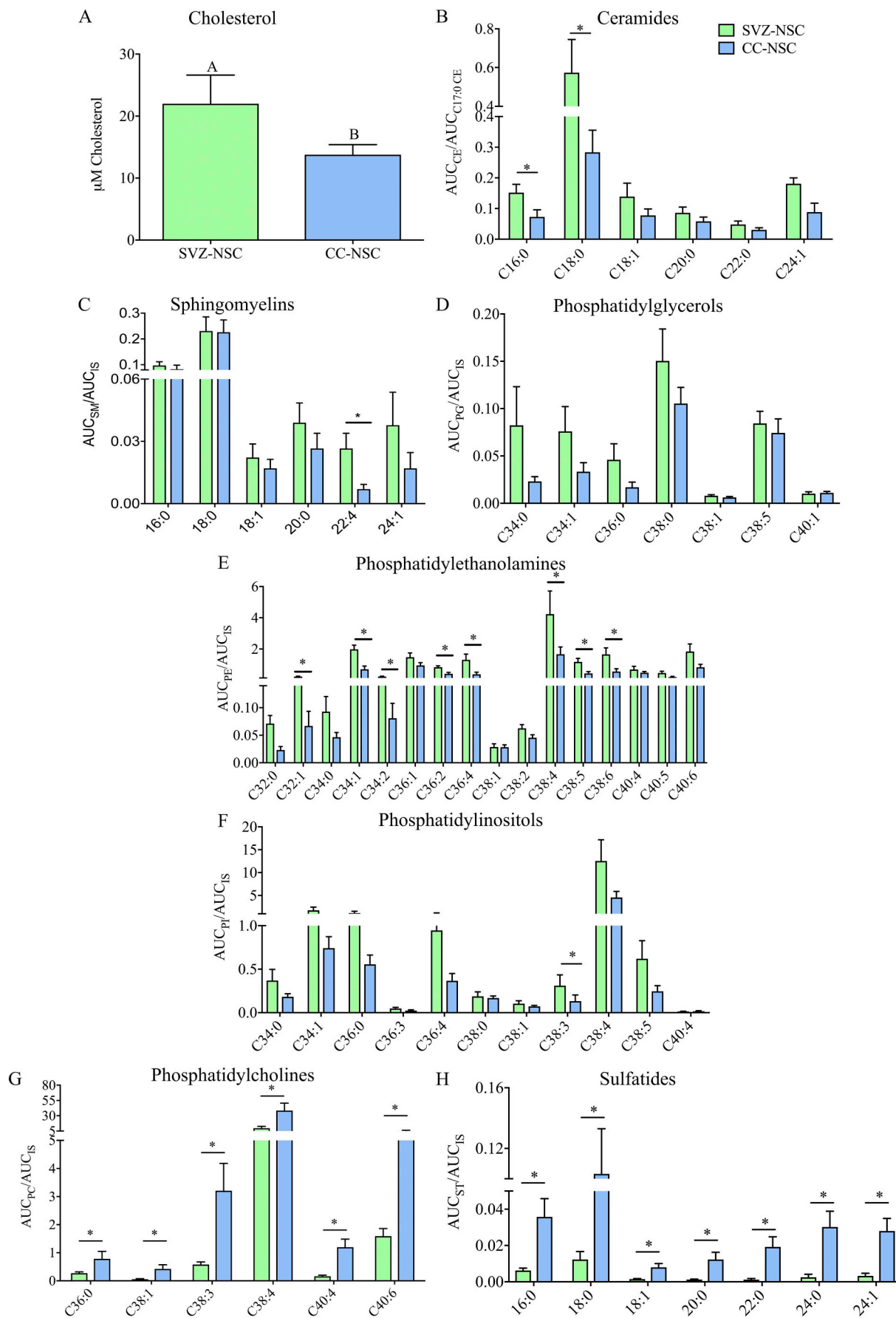
All the experiments were repeated at least 3 times. Error bars represent the standard error of the mean (SEM). The $p^* < 0.05$, $p^{**} < 0.01$ and $p^{***} < 0.001$ were calculated with Mann-Whitney test or one-way ANOVA with a Tukey's post-test by using Prism 7.00 (GraphPad software, San Diego, CA).

3. Results

3.1. Influence of neural stem cell origin on lipid plasma membrane composition

As NSC origin could impact NFL-LNC interactions with NSC, we compared the proportions of the main lipid components of SVZ- and CC-NSC plasma membranes.

The cholesterol concentration measured in SVZ-NSC membranes was 2-fold higher than in CC-NSC membranes (Fig. 1A). The proportion of ceramides, sphingomyelins, phosphatidylglycerols (PG), phosphatidylethanolamines (PE) and phosphatidylinositols (PI) was also higher in SVZ-NSC than in CC-NSC membranes (Fig. 1 B–F). Phosphatidylcholines (PC) and sulfatides were on the contrary present in higher proportions in CC-NSC than in SVZ-NSC plasma membranes (Fig. 1 G–



(caption on next page)

Fig. 1. Comparison of SVZ-NSC and CC-NSC lipid plasma membrane composition. A. Cholesterol quantification in neural stem cell plasma membranes performed by Amplex® Red Cholesterol Assay Kit. B-H. Relative levels of plasma membrane lipids in NSC plasma membranes measured by HPLC-MS. The error bars represent the standard error of the mean (SEM) ($N = 5$, $*p < .05$). For interpretation of the references to color in this figure legend, the reader is referred to the web version of this article.

H). In details, the proportion of C16:0 and C18:0 ceramides was significantly higher in SVZ-NSC than in CC-NSC, with C18:0 being the most abundant in both cells (Fig. 1B). Among the different sphingomyelins that were analyzed, 18:0 was the most abundant whatever the cell type, while only the proportion of 22:4 was significantly higher in SVZ-NSC membranes (Fig. 1C). PG were more abundant in SVZ-NSC than in CC-NSC but the differences were not significant (Fig. 1D). Seven PE were also in higher proportion in SVZ-NSC plasma membranes compared to CC-NSC membranes (Fig. 1E). Except for C32:0, C32:1, C34:0, C38:1 and 2, the other PE were equally represented. The same tendency was observed for PI with only C38:3 that was more abundant in SVZ-NSC than in CC-NSC (Fig. 1F). All the PC and sulfatides that were analyzed were more abundant in CC-NSC plasma membranes, with variable proportions (Fig. 1G-H). C38:4 and 18:0 were the most represented (PC and sulfatides, respectively).

3.2. Impact of ceramide and phosphatidylcholine proportions on liposome fluidity and their interactions with NFL-LNC

SVZ-NSC contained more ceramides while CC-NSC more PC. To study the impact of a higher ceramide content versus a higher PC content on liposome fluidity (GP of Laurdan), but also on the influence of liposome interaction with NFL-LNC on liposome GP, one liposome with high proportion of ceramides (Liposome 1 (Lip1), Table 1) and one with high amount of PC (Liposome 2 (Lip 2)) were produced and their GP were measured. The liposome composition was selected according to the diagram published by Silva et al. [25].

Lip 1 GP was significantly higher than Lip 2 GP (0.452 versus 0.203, respectively) (Fig. 2). Following incubation with NFL-LNC, GP of Lip 1 remained unchanged while GP of Lip 2 significantly increased, consistent with a rigidification of the liposome lipid bilayer.

3.3. Impact of NFL-LNC on liposome fluidity in function of their steady state fluidity

To determine whether steady state GP affected NFL-LNC impact on membrane fluidity, liposomes with different GP were prepared and incubated with NFL-LNC.

Nine liposomes with GP ranking between 0.619 and 0.150 (Fig. 3A)

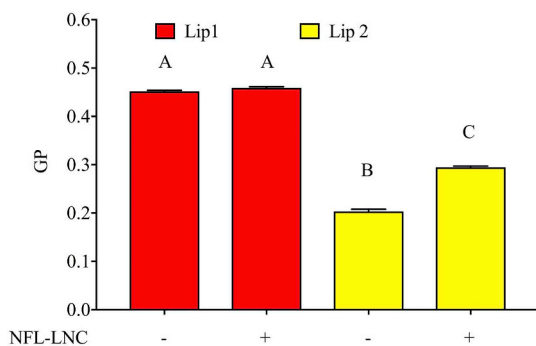


Fig. 2. Impact of ceramide and phosphatidylcholine proportions on liposome GP and on the influence of liposome interaction with NFL-LNC on liposome GP. Liposome 1 (Lip 1) contained a higher content of ceramide (60%) than Liposome 2 (Lip 2) (10%). GP were measured before (–) and after (+) 5-min incubation with NFL-LNC at 25 °C. Error bars represent the standard error of the mean (SEM) ($N = 3$, $n = 3$, conditions not linked by the same letter were significantly different, $p < .05$). For interpretation of the references to color in this figure legend, the reader is referred to the web version of this article.

were incubated with NFL-LNC. When liposomes were incubated with NFL-LNC, GP increased significantly for Lip 7 and 3 and significantly decreased for Lip 10, 5 and 8 (Fig. 3B). On one hand, NFL-LNC increased the fluidity of liposomes with a GP higher than 0.408, and the higher the steady-state liposome GP, the higher the fluidification effect. On the other hand, NFL-LNC significantly increased the rigidity of liposomes with a GP lower than 0.329, and the lower the steady-state liposome GP, the higher the rigidification effect of NFL-LNC. Regarding intermediate GP values ($0.329 \geq GP \leq 0.408$), no significant effect of NFL-LNC was observed on liposome's ΔGP . A linear correlation can be then established between liposome steady-state GP and the ΔGP induced by NFL-LNC (Fig. 3C). The lowest the steady-state GP, the lowest the ΔGP , with a rigidification of the liposome membrane for steady-state GPs up to 0.3926 and a fluidification for steady state GPs above that value.

3.4. Impact of NFL-LNC on neural stem cell fluidity

Then, the GP of SVZ- and CC-NSC before and after incubation with NFL-LNC was measured. GP of SVZ-NSC was significantly lower than GP of CC-NSC (0.313 versus 0.390, respectively) (Fig. 4). Incubation with NFL-LNC induced a significant increase of SVZ-NSC GP (+ 10%) and a decrease of CC-NSC GP (– 7%).

3.5. Sensitivity of neural stem cell membrane to NFL permeabilization effect

NFL is known to have a permeabilization effect on NSC [11]. In order to determine if SVZ- and CC-NSC were differently impacted by NFL, NSC were pre-incubated with increasing concentrations of NFL in presence of FITC-dextran (either 4 kDa or 10 kDa).

Only when SVZ-NSC were incubated with NFL 20 μM in presence of 4 kDa FITC-dextran an increase of cell permeability was observed (4.5-fold), while no significant effect was detected with 10 kDa FITC-dextran or when lower concentrations of NFL were used (Fig. 5A). This effect was not found when assessed on CC-NSC. These results were confirmed by confocal imaging, as only when SVZ-NSC were incubated with the highest concentration of NFL (20 μM) and with 4 kDa FITC-dextran, fluorescence could be visualized in the cells (Fig. 5B).

4. Discussion

We previously observed that NFL-LNC penetrate and co-localize with SVZ-NSC but not with CC-NSC [11]. The present study disclosed some of the factors modulating the interactions between NFL-LNC and SVZ-NSC while providing new information on NSC lipid plasma membrane composition and properties. We showed for the first time, to the best of our knowledge, that NSC origin impacts lipid composition of its plasmatic membrane as well as its fluidity and permeability. We also demonstrated that neural stem cell plasma membrane fluidity influenced interactions between LNC and NSC.

Lipids are key components of animal cell membranes in which they are present at different proportions that strongly depend on cell type. Proportions of cholesterol and some of the ceramides, sphingomyelins, PE, PI, sulfatides and PC were significantly different between SVZ- and CC-NSC. PC are the most abundant phospholipid in animals and represent a very high proportion of the outer leaflet of plasma membranes, forming the bulk structural element of membranes. PE, sphingomyelins and, to a lesser extend PI, are also major constituents of cell plasma membranes. PC and sphingomyelins are mostly located in the outer membrane whereas PE and PI are primarily found in the inner

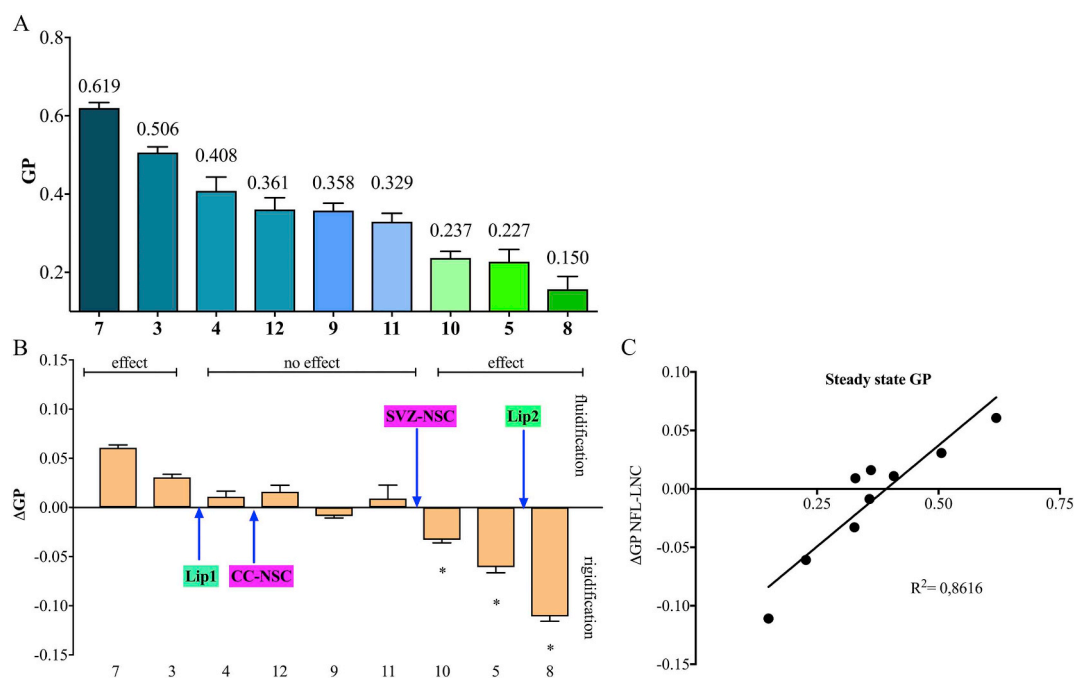


Fig. 3. Impact of NFL-LNC on liposome fluidity in function of their steady state GP. A. Liposomes were prepared with different ratios of POPC, eSM and Chol and their GP were measured. Liposomes were ranked from the higher to the lower GP (from the more rigid to the more fluid). B. Impact of NFL-LNC on liposome fluidity at 25 °C (Δ GP). Liposomes were presented based on their steady-state GP as for A. Blue arrows visualized Lip 1, Lip 2, SVZ-NSC and CC-NSC steady-state GP values, respectively. Error bars represent the standard error of the mean (SEM) ($N = 4$, $*p < .05$ versus steady state GP). C. Correlation between liposome steady-state GP and Δ GP induced by NFL-LNC. Egg sphingomyelin (eSM), 1-palmitoyl-2-oleoyl-*sn*-glycero-3-phosphocholine (POPC), and cholesterol (Chol). For interpretation of the references to color in this figure legend, the reader is referred to the web version of this article.

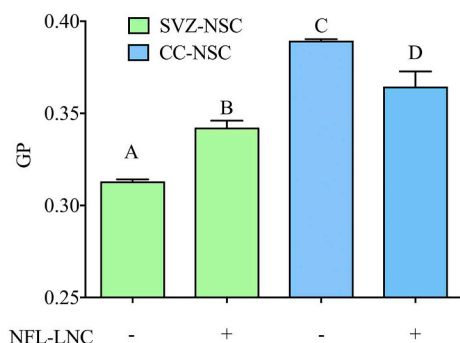


Fig. 4. Impact of NFL-LNC on neural stem cell membrane fluidity. SVZ-NSC and CC-NSC GP values, before (–) and after (+) 5-min incubation with NFL-LNC at 25 °C. Error bars represent the standard error of the mean (SEM) ($N = 4$, conditions not linked by the same letter were significantly different, $p < .05$). For interpretation of the references to color in this figure legend, the reader is referred to the web version of this article.

membrane. PC are cylindrical lipids, PE conical and PI inverted conical. Inclusion of PE in PC bilayers imposes a curvature stress onto the membrane as does the asymmetric distribution of various lipids between the two bilayer leaflets. As SVZ-NSC plasma membrane contained generally more PI, PE and sphingomyelins than CC-NSC membranes but less PC, NSC membranes could have different properties, including membrane curvature, depending of their origin. Because besides their shape lipids can be differentially charged and different lipid composition would also likely impact cell surface global charge. Lipid rafts are enriched in sphingolipids, such as sphingomyelins, and in cholesterol. As SVZ-NSC tend to contain more cholesterol and sphingomyelins and less PC, it might be hypothesized that SVZ-NSC contain more lipid rafts. All in all, plasma membranes of SVZ- and CC-NSC present distinct lipid compositions that could influence their interactions with NFL-LNC.

Lipids are involved in the modulation of many membrane properties. Since SVZ- and CC-NSC presented different lipid compositions, an impact on plasma membrane fluidity and permeability could be expected, thus resulting in changes of nanoparticle-cell interactions and penetration [26]. As ceramides were more abundant in SVZ-NSC and PC in CC-NSC, we produced liposomes either with high-ceramide (Lip 1) or high-PC (Lip 2) content to evaluate their role on membrane fluidity. Since our plasma membrane characterization gave us access to the relative abundance of lipids between SVZ- and CC-NSC, the composition of the liposomes may not consider the absolute amount of the lipids as well as the impact of peculiar micro-domains (e.g., lipid rafts) formed by specific ratio among the different lipid species. Nevertheless, liposomes can mimic many characteristics of a cellular membrane [27] and have previously been used as models to investigate the interactions between molecules/nanoparticles and cells [28,29]. Moreover, the GP of Laurdan, whose maximal emission depends on the polarity of the environment [30], allows the measurement of the effect of those interactions [31] by directly evaluating decrease/increase of GP or by calculating the Δ GP of the liposomes. GP is sensitive to the water content of lipid bilayer membranes. Consequently, this parameter can be used to determine the relative amount of solid and liquid phases in plasma membranes. The decrease of GP is typically associated with lower bilayer packing (increase of membrane fluidity) whereas an increase of GP corresponds to higher bilayer packing (increase of membrane rigidity); Δ GP variations must be interpreted conversely [32]. Ceramides are known to increase the rigidity of lipid membranes [33] while PC their fluidity [34]. As expected, the GP of Lip 1 was significantly higher compared to the GP of Lip 2 but, interestingly, only Lip 2 GP was impacted by NFL-LNC. Consequently, even if the proportion of these particular lipids played a role in interactions with NFL-LNC, lipids were not the only parameter that influence them.

As steady state GP of Lip 1 and 2 were significantly different, we hypothesized that NSC plasma membrane fluidity might influence NSC interactions with NFL-LNC. To study how membrane fluidity could be

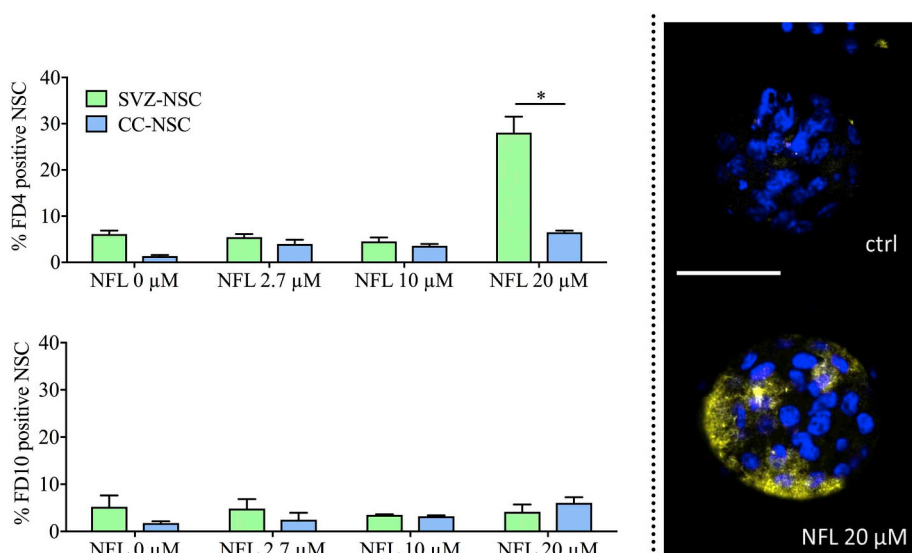


Fig. 5. Impact of NFL on NSC permeability. A. Percentage of NSC positive for 4 kDa and 10 kDa FITC dextran (FD4 and FD10) after incubation with increasing concentrations of NFL (0, 2.7, 10, 20 μM). Error bars represent the standard error of the mean (SEM) ($N = 3$, $p^* < 0.05$). B. Visualization of NFL permeabilization effect of SVZ-NSC by confocal imaging (20 μM, FD4) (blue: cell nucleus, yellow: FD4). Scale bar = 50 μm. For interpretation of the references to color in this figure legend, the reader is referred to the web version of this article.

modified by NFL-LNC, we prepared liposomes with different ratios of phosphatidylcholine (POPC), sphingomyelin (eSM) and cholesterol (Chol) (frequently used to mimic general eukaryotic plasma membranes [22]), and thus different GP. We showed that both the magnitude and the impact on membrane fluidity (i.e., fluidification or rigidification) induced by NFL-LNC correlated with the steady state fluidity of the liposomes, while no trend related to the lipid composition was observed. A linear correlation was indeed observed between steady state GP and ΔGP induced by incubation with NFL-LNC. Moreover, when placing Lip 1 and Lip 2 steady state GP on Fig. 3B, it appeared that Lip 1 was in the “no effect” zone while Lip 2 was in the “rigidification effect” zone, which correlated with the results observed in Fig. 2. Hence, fluidity is an important factor driving interaction between NFL-LNC and NSC. Then, we wanted to determine if this was also true for NSC. Surprisingly, SVZ-NSC plasma membrane, despite having more ceramides than CC-NSC, was significantly more fluid at steady state than CC-NSC plasma membrane, that yet had a higher proportion of PC. This suggests that although lipid composition plays an important role in cell membrane fluidity, it was not the only parameter driving NSC membrane fluidity. Nevertheless, when incubated with NFL-LNC, SVZ-NSC GP, located in the “rigidification effect range” (Fig. 3), increased while CC-NSC GP, located in the “fluidification effect range”, decreased. These results showed a correspondence between observations made with liposomes and NSC and supported the hypothesis that steady state fluidity of a lipid bilayer membrane influenced NFL-LNC impact on fluidity, and thus its interactions with cells.

In our previous work [11] we showed that NFL penetration into SVZ-NSC was not affected by energetic conditions (i.e., ATP depletion) while it significantly decreased at 4 °C in CC-NSC. With the current study we additionally showed that the peptide significantly increased the permeability of SVZ-NSC plasma membrane while it had no effect on CC-NSC. Interestingly, the higher amount of ceramides and the higher concentration of cholesterol measured in SVZ-NSC plasma membranes did not hinder the permeabilizing effect of the peptide NFL despite the fact that these conditions typically decrease fluidity and permeability of plasma membrane respectively [26,35]. Pae et al. showed that ceramides increase the uptake of arginine-rich cell-penetrating peptides (CPP) while preventing the internalization of amphipathic CPP [36,37]. In addition, Hecce et al. demonstrated that arginine-rich peptides can destabilize the plasma membrane by producing pores [38]. Since NFL contains arginines, we can hypothesize that the higher proportion of ceramides in SVZ-NSC could lead to an increased penetration of NFL into SVZ-NSC (i.e., at 4 °C) and to an increased permeability towards small molecules (i.e., FD4) compared to CC-NSC.

We do not exclude that what has been observed for NFL might be true for other arginine-rich peptides but we have no insight on such peptides and NSC.

Although this work provides compelling evidence for the crucial importance of NSC plasma membrane fluidity on their specific interactions with NFL-LNC, other parameters, such as protein composition and, consequently, membrane curvature, could certainly be responsible for the specific interactions of NFL-LNC with SVZ-NSC and thus would require further studies.

5. Conclusion

The objective of this study was to determine whether lipid composition, fluidity and permeability of NSC plasma membrane could explain the specific targeting of SVZ-NSC by NFL-LNC. We showed that membrane fluidity could impact the interactions between nanomedicines and cells. Also, the characterization of the lipid composition of NSC plasma membranes provided important information highlighting an origin-dependent composition and fluidity of NSC. Although the present study clearly establishes the role of plasma membrane fluidity, it would be interesting to look into the impact of other parameters, such as plasma membrane and cytoskeleton protein composition.

Acknowledgments

Dario Carradori was supported by NanoFar “European Doctorate in Nanomedicine” EMJD programme funded by EACEA. This work was supported by grants from the Walloon Region (AEROGAL 1318023), Université catholique de Louvain (F.S.R) and Fonds National de la Recherche Scientifique (F.R.S.-FNRS). A. des Rieux is a F.R.S.-FNRS Research Associate. The MASSMET platform is acknowledged for the access to the HPLC-MS.

Declarations of interest

None.

References

- [1] C.A. Herberts, M.S.G. Kwa, H.P.H. Hermesen, Risk factors in the development of stem cell therapy, *J. Transl. Med.* 9 (2011) 29.
- [2] O.E. Simonson, A. Domogatskaya, P. Volchkov, S. Rodin, The safety of human pluripotent stem cells in clinical treatment, *Ann. Med.* 47 (5) (2015) 370–380.
- [3] C. Xie, D. Cong, X. Wang, Y. Wang, H. Liang, X. Zhang, Q. Huang, The effect of simvastatin treatment on proliferation and differentiation of neural stem cells after

- traumatic brain injury, *Brain Res.* 1602 (2015) 1–8.
- [4] C. Saraiva, J. Paiva, T. Santos, L. Ferreira, L. Bernardino, MicroRNA-124 loaded nanoparticles enhance brain repair in Parkinson's disease, *J. Control. Release* 235 (2016) 291–305.
- [5] L.-C.C. Barreau Kristell, Eyer Joel, Review of clinical trials using neural stem cells, *JSM Biotechn. Biomed. Eng.* 3 (3) (2016) 1057.
- [6] A. Bocquet, R. Berges, R. Frank, P. Robert, A.C. Peterson, J. Eyer, Neurofilaments bind tubulin and modulate its polymerization, *J. Neurosci.* 29 (35) (2009) 11043–11054.
- [7] C. Lépinoux-Chambaud, K. Barreau, J. Eyer, The neurofilament-derived peptide NFL-TBS. 40-63 targets neural stem cells and affects their properties, *Stem Cells Transl. Med.* 5 (7) (2016) 901–913.
- [8] R. Berges, J. Balzeau, A.C. Peterson, J. Eyer, A tubulin binding peptide targets glioma cells disrupting their microtubules, blocking migration, and inducing apoptosis, *Mol. Ther.* 20 (7) (2012) 1367–1377.
- [9] C. Lépinoux-Chambaud, J. Eyer, The NFL-TBS. 40-63 anti-glioblastoma peptide enters selectively in glioma cells by endocytosis, *Int. J. Pharm.* 454 (2) (2013) 738–747.
- [10] J. Balzeau, M. Pinier, R. Berges, P. Saulnier, J.-P. Benoit, J. Eyer, The effect of functionalizing lipid nanocapsules with NFL-TBS. 40-63 peptide on their uptake by glioblastoma cells, *Biomaterials* 34 (13) (2013) 3381–3389.
- [11] D. Carradori, P. Saulnier, V. Pr eat, A. Des Rieux, J. Eyer, NFL-lipid nanocapsules for brain neural stem cell targeting in vitro and in vivo, *J. Control. Release* 238 (2016) 253–262.
- [12] N.T. Huynh, C. Passirani, P. Saulnier, J.-P. Benoit, Lipid nanocapsules: a new platform for nanomedicine, *Int. J. Pharm.* 379 (2) (2009) 201–209.
- [13] W. Guo, N.E. Patzlaff, E.M. Jobe, X. Zhao, Isolation of multipotent neural stem or progenitor cells from both the dentate gyrus and subventricular zone of a single adult mouse, *Nat. Protoc.* 7 (11) (2012) 2005.
- [14] J.-P. Hugnot, Isolate and culture neural stem cells from the mouse adult spinal cord, *Neural Progenitor Cells*, Springer, 2013, pp. 53–63.
- [15] M. Faiz, N. Sachewsky, S. Gasc on, K.A. Bang, C.M. Morshead, A. Nagy, Adult neural stem cells from the subventricular zone give rise to reactive astrocytes in the cortex after stroke, *Cell Stem Cell* 17 (5) (2015) 624–634.
- [16] J.M. Suski, M. Lebedzinska, A. Wojtala, J. Duszynski, C. Giorgi, P. Pinton, M.R. Wieckowski, Isolation of plasma membrane-associated membranes from rat liver, *Nat. Protoc.* 9 (2) (2014) 312.
- [17] V. Mutemberezi, J. Masquelier, O. Guillemot-Legr is, G.G. Muccioli, Development and validation of an HPLC-MS method for the simultaneous quantification of key oxysterols, endocannabinoids, and ceramides: variations in metabolic syndrome, *Anal. Bioanal. Chem.* 408 (3) (2016) 733–745.
- [18] O. Guillemot-Legr is, J. Masquelier, A. Everard, P.D. Cani, M. Alhouayek, G.G. Muccioli, High-fat diet feeding differentially affects the development of inflammation in the central nervous system, *J. Neuroinflammation* 13 (1) (2016) 206.
- [19] M. Hope, M. Bally, G. Webb, P. Cullis, Production of large unilamellar vesicles by a rapid extrusion procedure. Characterization of size distribution, trapped volume and ability to maintain a membrane potential, *Biochimica et Biophysica Acta (BBA)-Biomembranes* 812 (1) (1985) 55–65.
- [20] G.R. Bartlett, Phosphorus assay in column chromatography, *J. Biol. Chem.* 234 (3) (1959) 466–468.
- [21] T.P. Etzerodt, S. Trier, J.R. Henriksen, T.L. Andresen, A GALA lipopeptide mediates pH- and membrane charge dependent fusion with stable giant unilamellar vesicles, *Soft Matter* 8 (21) (2012) 5933–5939.
- [22] A. Cuco, A.P. Serro, J.P. Farinha, B. Saramago, A.G. da Silva, Interaction of the alzheimer A β (25–35) peptide segment with model membranes, *Colloids Surf. B: Biointerfaces* 141 (2016) 10–18.
- [23] T. Parasassi, G. De Stasio, G. Ravagnan, R. Rusch, E. Gratton, Quantitation of lipid phases in phospholipid vesicles by the generalized polarization of Laurdan fluorescence, *Biophys. J.* 60 (1) (1991) 179–189.
- [24] B. Heurtaut, P. Saulnier, B. Pech, J. Proust, J. Richard, J. Benoit, Lipidic Nanocapsules: Preparation Process And Use As Drug Delivery Systems, WOO2688000 (2000).
- [25] L. Silva, R.F. De Almeida, A. Fedorov, A.P. Matos, M. Prieto, Ceramide-platform formation and-induced biophysical changes in a fluid phospholipid membrane, *Mol. Membr. Biol.* 23 (2) (2006) 137–148.
- [26] C. Peetla, S. Vijayaraghavalu, V. Labhasetwar, Biophysics of cell membrane lipids in cancer drug resistance: implications for drug transport and drug delivery with nanoparticles, *Adv. Drug Deliv. Rev.* 65 (13–14) (2013) 1686–1698.
- [27] A. Bangham, M. Hill, N. Miller, Preparation and use of liposomes as models of biological membranes, *Methods in Membrane Biology*, Springer, 1974, pp. 1–68.
- [28] J. Kristl, B. Volk, P. Ahlin, K. Gomba c, M. Šentjurc, Interactions of solid lipid nanoparticles with model membranes and leukocytes studied by EPR, *Int. J. Pharm.* 256 (1–2) (2003) 133–140.
- [29] G. Van Meer, D.R. Voelker, G.W. Feigenson, Membrane lipids: where they are and how they behave, *Nat. Rev. Mol. Cell Biol.* 9 (2) (2008) 112.
- [30] D.M. Owen, C. Rentero, A. Magenau, A. Abu-Siniyeh, K. Gaus, Quantitative imaging of membrane lipid order in cells and organisms, *Nat. Protoc.* 7 (1) (2012) 24.
- [31] E. Kov acs, T. Savopol, M.-M. Iordache, L. S apl acan, I. Sobaru, C. Istrate, M.-P. Mingeot-Leclercq, M.-G. Moiesescu, Interaction of gentamicin polycation with model and cell membranes, *Bioelectrochemistry* 87 (2012) 230–235.
- [32] L. Bagatolli, LAURDAN fluorescence properties in membranes: a journey from the fluorometer to the microscope, *Fluorescent Methods to Study Biological Membranes*, Springer, 2012, pp. 3–35.
- [33] E.R. Catapano, L.R. Arriaga, G. Espinosa, F. Monroy, D. Langevin, I. L opez-Montero, Solid character of membrane ceramides: a surface rheology study of their mixtures with sphingomyelin, *Biophys. J.* 101 (11) (2011) 2721–2730.
- [34] Y. Yawata, *Cell Membrane: The Red Blood Cell as a Model*, John Wiley & Sons, 2006.
- [35] M. Brabec, D. Schober, E. Wagner, N. Bayer, R.F. Murphy, D. Blaas, R. Fuchs, Opening of size-selective pores in endosomes during human rhinovirus serotype 2 in vivo uncoating monitored by single-organelle flow analysis, *J. Virol.* 79 (2) (2005) 1008–1016.
- [36] J. Pae, P. S a alik, L. Liivam agi, D. Lubenets, P. Arukuusk,  . Langel, M. Pooga, Translocation of cell-penetrating peptides across the plasma membrane is controlled by cholesterol and microenvironment created by membranous proteins, *J. Control. Release* 192 (2014) 103–113.
- [37] M.B. Lande, J.M. Donovan, M.L. Zeidel, The relationship between membrane fluidity and permeabilities to water, solutes, ammonia, and protons, *J. General Physiol.* 106 (1) (1995) 67–84.
- [38] H. Herce, A. Garcia, J. Litt, R. Kane, P. Martin, N. Enrique, A. Rebolledo, V. Milesi, Arginine-rich peptides destabilize the plasma membrane, consistent with a pore formation translocation mechanism of cell-penetrating peptides, *Biophys. J.* 97 (7) (2009) 1917–1925.